ELSEVIER

Journal of Alloys and Compounds 356–357 (2003) 447–451

Journal of ALLOYS AND COMPOUNDS

www.elsevier.com/locate/jallcom

Protium absorption–desorption properties of Ti–Cr–Mo bcc solid solution alloys

A. Kamegawa*, T. Tamura, H. Takamura, M. Okada

Department of Materials Science, Graduate School of Engineering, Tohoku University, Sendai 980-8579, Japan

Received 10 June 2002; accepted 25 October 2002

Abstract

We have investigated the protium absorption–desorption properties of Ti–Cr–Mo alloys of varying composition, including cycling-induced effects. The capacity of alloys with less than 10 at% Mo has an H/M ratio of 1.8 at 10 MPa hydrogen pressure, and remains almost unchanged regardless of Mo content. The 40Ti–Cr–2.5Mo alloy has the widest plateau region observed in this study. The amount of protium desorption and the mean particle size vary inversely with the logarithm of cycle number up to 300 cycles. The capacity of the alloy is drastically affected by the conditions of cycling. With longer evacuation times the capacity decreases significantly. The lattice parameter of the β protide increases with increasing cycles, and the reflection peaks in XRD studies are broadened. The reduction in capacity after several absorption–desorption cycles is somewhat restored by annealing at 673 K for 2 h under vacuum. The absorption pressure of the plateau for the 101st cycle, after annealing following the 100th cycle, recovers to that of the plateau for the first cycle, but then decreases with additional cycling.

Keywords: Body centered cubic; Solid solution alloys; Hydrogen storage alloy; Protium; PCT isotherm

1. Introduction

Recent interest in hydrogen fuel cell power for emission-free vehicles has driven the investigation of high capacity protium absorbing alloys for hydrogen storage. The use of such alloys offers several advantages, including compactness, safety, and freedom from shape constraints. A likely candidate for the purpose is a Ti- or V-based solid solution alloy with a body centered cubic (bcc) structure.

Vanadium [1] or V-based solid-solutions with a bcc structure are known to absorb about 3.8 mass% (H/M~2) of protium (hydrogen atom) around ambient temperature. Iba and Akiba [2–4] reported that multi-phase Ti–V–Mn alloys consisting of Laves and bcc solid-solution phases had good desorption capacities of nearly 2.1 mass% H. Iba and Akiba [2,5] also reported that a Ti–40at%V–35at%Cr alloy with a bcc structure could desorb about 2.4 mass% protium. We have investigated varying compositions and heat-treatment conditions to increase the protium capacities of Ti–Cr–V alloys [6–19]. The optimum heat-treatment conditions for this alloy were reported to be annealing at 1573 K for 1 min, followed by quenching in water. Okada et al. [6] reported that the Ti–Cr–V alloys with low V content (5–7.5 at% V) yield a high capacity of nearly 3 mass% protium, which is the highest value reported so far at 313 K. The optimum composition of the Ti–Cr–V alloys was also discussed and the alloys with Ti/Cr ratio of 2/3 have a plateau region in their PCT curve around 0.1 MPa (1 atm) with the highest capacity at 313 K. These alloys are promising since they contain a relatively low amount of expensive vanadium. Since the bcc alloys with low V content exhibit high capacities comparable to pure vanadium or V-based alloys, we surmised that V-free Ti–Cr alloys with a bcc structure might also exhibit a high capacity. The equilibrium phase of the Ti–Cr system has a bcc solid-solution in a high and narrow range below the congruent melting point. Therefore, it is difficult to obtain only bcc phase freezing from high temperature in the binary alloys. Recently, we reported that the addition of Mo to Ti–Cr alloys stabilizes the bcc phase in the binary phase diagram, and that adding Mo to Ti–Cr alloys gives

*Corresponding author.
E-mail address: kamegawa@material.tohoku.ac.jp (A. Kamegawa).

0925-8388/02/$ – see front matter
doi:10.1016/S0925-8388(02)01239-2

not only flattened plateau regions, but also capacities of 3.6 mass% protium similar to Ti–Cr–V alloys [14].

Here we report the protium absorption–desorption properties of Ti–Cr–Mo alloys with varying Mo content and Ti/Cr ratio. The cyclic properties of the alloys are also investigated.

2. Experimental procedures

The alloys were prepared from raw materials by arc melting on a water-cooled copper hearth under pure argon. The purity of the elements was as follows: Ti>99.6 at% and Cr, Mo>99.99 at%. In our previous study, the Ti–Cr–V alloys with added Mo were mainly bcc phase. However, Mo or unmelted additives tended to remain in the alloys with more than 10% Mo, because of molybdenum's comparatively high melting point (2883 K). Therefore, Cr–Mo alloys were melted first, and then Ti–Cr–Mo alloys were prepared. Sample ingots were remelted three times to ensure their homogeneity. To obtain the bcc phase in the alloys and enhance their homogeneity, the samples were annealed at 1673 K for 1 min, and quenched in ice water.

Crystal structures and lattice parameters were studied with an X-ray diffractometer (XRD) using Cu Kα radiation. PCT curves were measured with a Sieverts-type apparatus at 313 K. Each sample was put into a vessel and was evacuated at 313 K for 2 h, using a rotary vacuum pump. The alloys absorb protium fully at the first hydrogen charge process, so initial activation treatments were unnecessary. Hydrogen was introduced gradually into the vessel up to a pressure of 10 MPa. Accelerated cyclic experiments were carried out by holding the sample for 30 min at 10 MPa H_2, followed by evacuation for 1 or 30 min. The evacuation for 30 and 1 min correspond to reducing the hydrogen equilibrium pressure to less than 0.001 and 0.07 MPa, respectively, and were called 'cycle A' and 'cycle B', respectively. The mean particle size of the powder samples after the cyclic experiments was measured with a laser diffraction particle size analyzer.

3. Results and discussion

Fig. 1 shows PCT curves of Ti–(60−x)Cr–xMo heat-treated alloys (x=2.5, 5, 10, 20, 30, 50). XRD shows only the bcc phase. The pressure of the plateau for these alloys increases with increasing Mo content. The H/M ratio of the alloy with less than 10 at% Mo is as high as 1.8 at 10 MPa hydrogen pressure and does not vary with Mo content. However, the H/M ratio of the alloy with more than 20 at% Mo decreases with increasing Mo content, and the slope of the plateau increases. Furthermore, the mass concentration of absorbed protium decreases with increasing Mo content. The mass absorbing capacity rises to a maximum value of 3.6 mass% when the Mo content is 2.5% Mo, and then decreases with increasing Mo content.

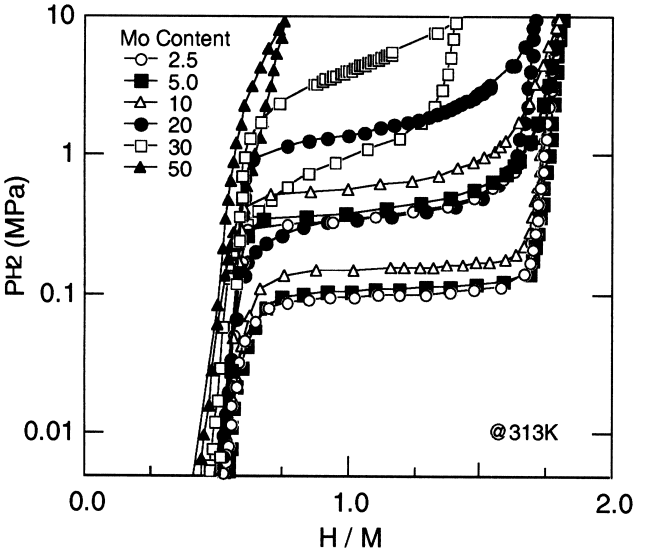

Fig. 1. PCT curves of Ti–(60−x)Cr–xMo alloys (x=2.5, 5, 10, 20, 30, 50).

Fig. 2 shows PCT curves of xTi–Cr–2.5Mo alloys (x=37, 39, 40, 41, 43). XRD showed that alloys with more than 39% Ti consist mainly of the bcc phase, but the 37% Ti alloy contains the bcc phase as a major phase and Laves phase as a minor one, which is known to absorb a small amount of protium at around room temperature. Alloys containing more than 40% Ti absorb protium up to an H/M of 1.8, but the capacities of the alloys with less than 39% Ti decrease with decreasing Ti content. The plateau pressures of the alloys decrease with increasing Ti content, and the 40Ti–Cr–2.5Mo alloy has the widest plateau region in this study.

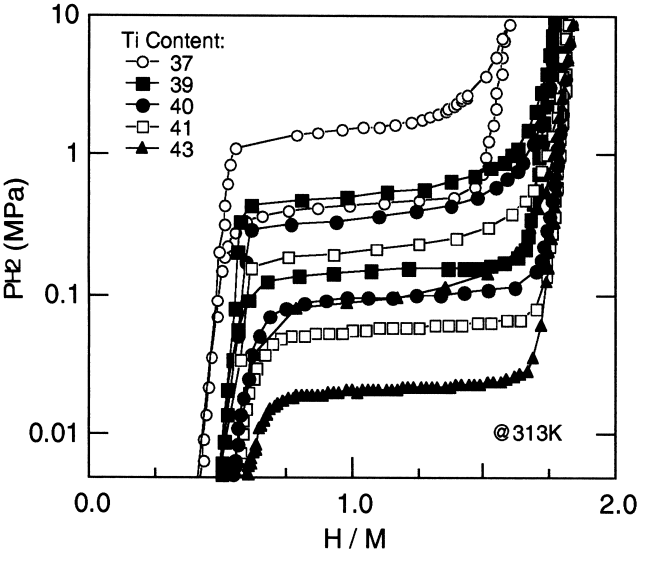

Fig. 2. PCT curves of xTi–(60−x)Cr–2.5Mo alloys process (x=37, 39, 40, 41, 43).

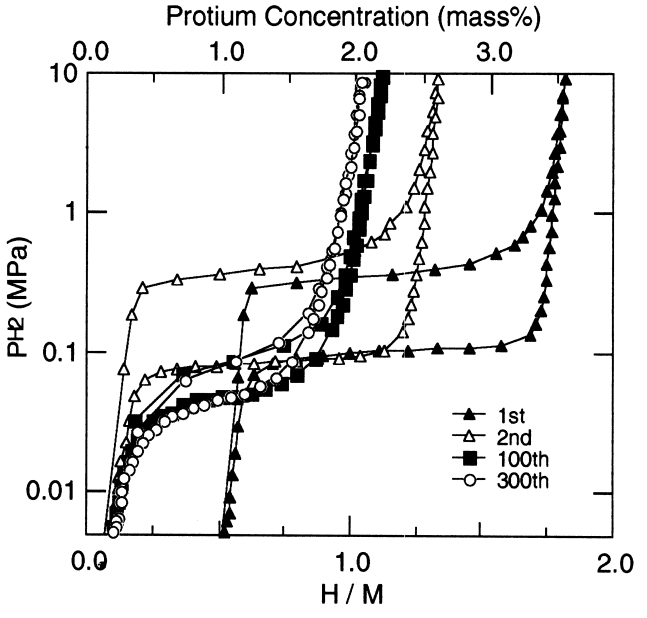

Fig. 3. PCT curves of 40Ti–Cr–2.5Mo alloys for the first, second, 100th, and 300th cycles of Cycle A (10 MPa H_2 for 30 min, then evacuation for 30 min before each measurement).

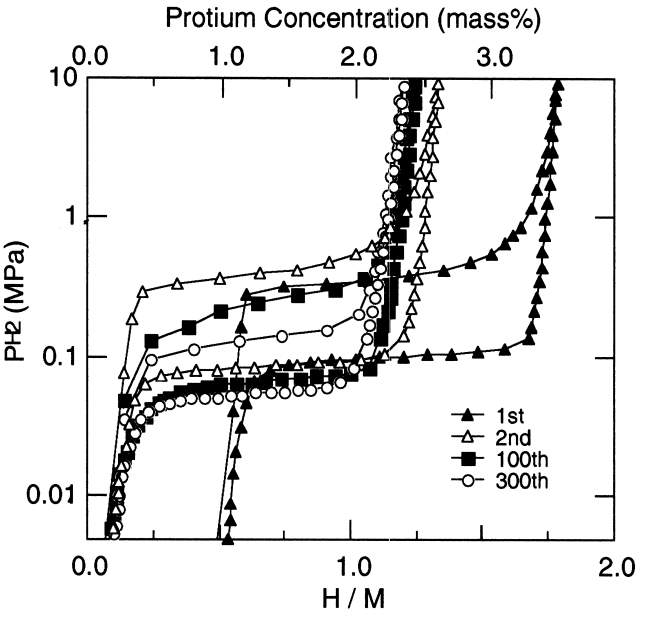

Fig. 4. PCT curves of 40Ti–Cr–2.5Mo alloys for the first, second, 100th, and 300th cycles of Cycle B (10 MPa H_2 for 30 min, then evacuation for 1 min before each measurement).

Fig. 3 shows PCT curves of the 40Ti–Cr–2.5Mo alloy for the first to 300th cycle of cycle A (with a thorough desorbing stage). The reason for the large difference of reversible capacities between PCT curves for the first and second cycle is the resetting of the origin of the protium concentration before the second cycle measurement. While the desorption pressure of the plateau decreases slightly from the first to second cycle, the absorption pressure increases significantly. This phenomenon was also observed for the other alloys in this study. However, both the plateau pressure of the alloy and the reversible capacity decrease drastically beyond the second cycle, with a reduction from an H/M of 1.3 for the second cycle to 1.0 for the 300th cycle. The hysteresis of the curve becomes smaller as the number of cycles increases.

Fig. 4 shows PCT curves of 40Ti–Cr–2.5Mo alloy after undergoing cycle B, with its comparatively smaller desorbing process. Compared with the results in Fig. 3, the decrease in plateau pressure is small and the reversible capacity is large. Although the slope of the desorption plateau does not depend to any significant degree on the number of cycles, the plateau region of the absorption curve declines slightly. The protium concentration of β protide after the absorption–desorption process of cycle B is larger than the concentration after cycle A, as mentioned above. The difference after cycle A and cycle B is the amount of protium in β protide, and the lattice parameter of β protide after cycle A is smaller than that after cycle B. Cycle A may cause greater expansion and contraction of the lattice with β–γ transformation than cycle B. After cycle A, the sample experiences larger lattice stress than that after cycle B. It seems likely that the protium concentration of β protide in the absorption–desorption cycle may cause a decrease of capacity and differently shaped PCT curves for cycles A and B.

Fig. 5 shows changes in the amount of desorption (a), the absorption and desorption pressure of the plateau (b), and mean particle size (c) versus the number of cycles. The open and closed circles (○ and ●) in the figure represent the absorption and desorption processes, respectively, after several repetitions of cycle A. The open and closed triangles (△ and ▲) represent the absorption and desorption processes, respectively, after several repetitions of cycle B. The amount of desorption is defined as the difference in the protium concentration at desorption between 7 and 0.01 MPa. The desorption and the mean particle size vary inversely with the logarithm of the cycle number up to 300 cycles. The particle size decreases from 1 to 2 mm before hydrogenation to less than 50 μm after the first cycle. Under cycle A conditions, the decrement of absorption pressure up to the 20th cycle is larger than that of desorption. To investigate the relationship between capacity and particle size, we determined the PCT curve of a sample with a mean particle size of about 13.8 μm (obtained by grinding under Ar). We found that the capacity does not directly depend on the particle size of the alloys.

Fig. 6 shows XRD patterns of the 40Ti–Cr–2.5Mo alloy after PCT measurement for several cycles. All samples contain about 0.5 H/M of residual protium after PCT measurement. All samples have only a β protide phase with a bcc structure. It was previously reported that the Ti–Cr–Mo alloys transform from the α phase as protium solid solutions with a bcc structure, via a β protide phase

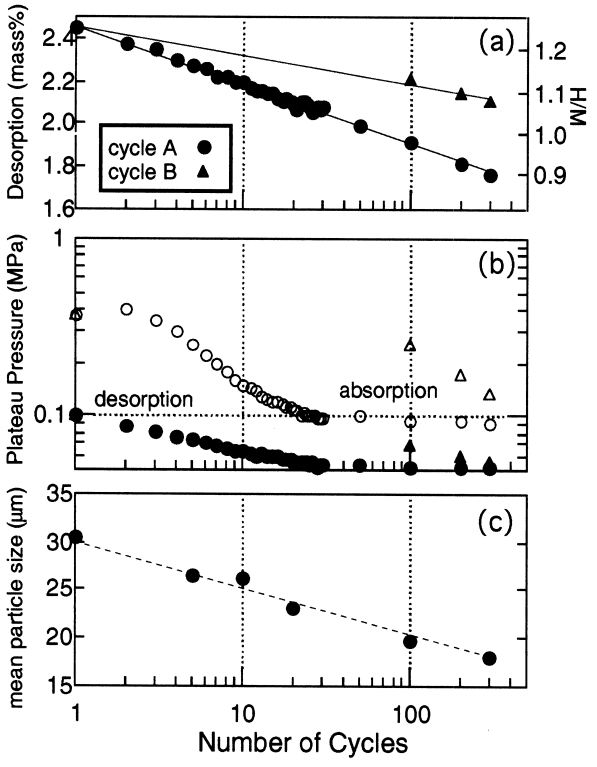

Fig. 5. Changes in desorption (a), the absorption and desorption pressure of the plateau (b), and mean particle size (c) versus the number of cycles. Open and closed circles (○ and ●) indicate the absorption and desorption processes, respectively, measured after several repetitions of cycle A. Open and closed triangles (△ and ▲) represent absorption and desorption processes, respectively, after several repetitions of cycle B. (The amount of desorption is defined as the difference in protium concentration on desorption between 7 and 0.01 MPa.).

as mono protide with a bcc to a γ protide phase as di-protide with a fcc structure [14]. The lattice parameter and the width of the peaks increase with the number of cycles. Compared with intermetallic compounds, generally, V- or Ti-based solid solution alloys with a bcc structure show a comparatively large hysteresis. The Ti–Cr–Mo alloys in this study also have a large hysteresis for the first few cycles, but the hysteresis decreases significantly with increasing cycles as shown in Fig. 5. It is well known that lattice defects and dislocations are easily generated by transformation of the crystal structure or grain deformation, so the large hysteresis of the bcc alloys may be caused by the generation of numerous defects and dislocations during the absorption process. The drastic decrement of absorption pressure could be caused by an increase in lattice defects or dislocation density, considering the broadened peak in the XRD patterns. It seems likely that such defects act as protium trapping sites. Thus the increment in lattice parameter due to cycling suggests that the desorbable protium in PCT measurements decreases with increasing cycles and an associated increase in protium trapping sites.

In order to fully dehydrogenate the sample after the measurement, it was annealed under vacuum at 673 K for 2 h. Fig. 7 shows PCT curves of the 40Ti–Cr–2.5Mo alloy for the first, 100th, 101st, and 150th cycles (annealing followed the 100th cycle). The amount of desorption between 7 MPa and 0.01 MPa increased from ~1.0 H/M at the 100th cycle to 1.1 H/M at the 101st, after annealing. Thus it is likely that the trapped protium is desorbed from the lattice defects. The absorption pressure of the plateau for the 101st cycle recovered to nearly equal that of the first cycle, but subsequently decreased with additional cycling. On the other hand, the desorption pressure for the 101st cycle is higher than the pressure for the first cycle, and the pressure does not significantly decrease with

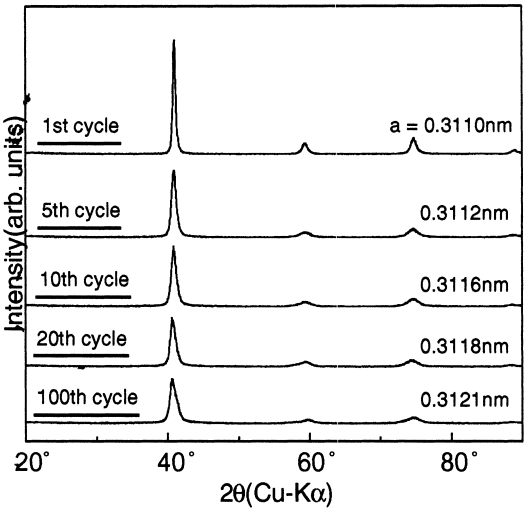

Fig. 6. XRD patterns of 40Ti–Cr–2.5Mo after PCT measurement for several cycles.

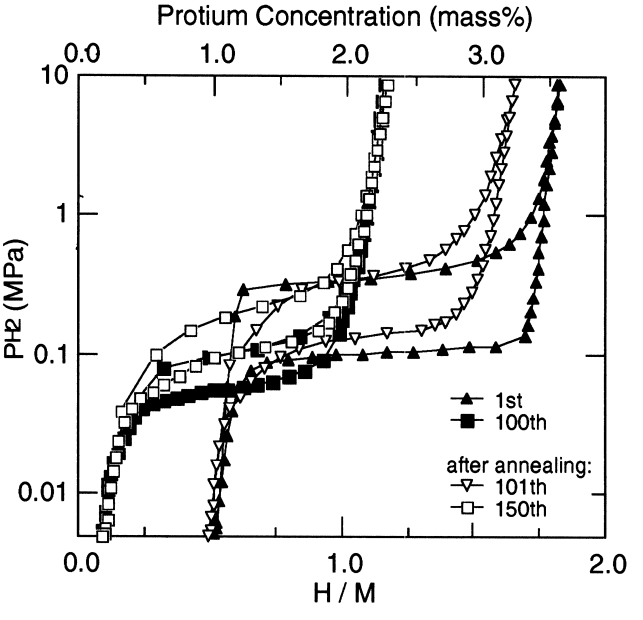

Fig. 7. PCT curves of the 40Ti–Cr–2.5Mo alloy. Samples were annealed under vacuum at 673 K for 2 h after the 100th cycle and before the 150th cycle.

cycling after the 101st cycle. Therefore, the recovery of the absorption pressure of the plateau by annealing may be due to the fact that some accumulated lattice defects induced by absorption–desorption cycles were annealed out. Later, dislocations are again generated in the alloys by subsequent absorption–desorption cycles. XRD shows that the broadened diffracted peaks are unchanged by the annealing after the 100th cycle. Thus it can be conjectured that the origin of decreasing capacity with cycling is not only due to the increase in undesorbable sites, but also a decrease in absorbable sites, considering the results shown in Fig. 4. It is important to clarify the effect of the protium concentration in the β protide phase on the cyclic properties of the alloys.

4. Conclusions

We performed a systematic characterization of the PCT isotherms for Ti–Cr–Mo alloys with varying composition and cyclic changes, and drew the following conclusions.

The highest capacity found in this study was 1.8 H/M, and no change in the H/M ratio of the alloy was observed with less than 10 at% Mo content. The 40Ti–Cr–2.5Mo alloy had the widest plateau region in this study.

The amount of protium desorption and the mean particle size decrease linearly versus the logarithm of the cycle number, up to the 300th cycle.

The decrement of absorption pressure up to cycle 20 is larger than that of the desorption, and the hysteresis becomes smaller. XRD indicates that the lattice parameter of the β protide phase increases with increasing number of cycles, and the XRD reflection peaks are broadened. The decreased capacity after several absorption–desorption cycles is slightly restored by annealing under vacuum at 673 K for 2 h. The absorption pressure of the plateau for the 101st cycle (after annealing following the 100th) recovers to that of the plateau for the first cycle, but decreases again with cycling.

References

[1] J.J. Reilly, R.H. Wiswall, Inorg. Chem. 9 (1970) 1678–1682.
[2] H. Iba, E. Akiba, J. Alloys Comp. 253 (1997) 21–24.
[3] H. Iba, E. Akiba, J. Alloys Comp. 231 (1995) 508–512.
[4] H. Iba, Ph.D. Dissertation, Tohoku Univ. Japan (1997), in Japanese.
[5] E. Akiba, H. Iba, Intermetallics 6 (1998) 461–470.
[6] M. Okada, T. Kuriiwa, T. Tamura, H. Takamura, A. Kamegawa, Metals Mater. Korea 7 (2001) 67–72.
[7] Y. Tominaga, S. Nishimura, T. Amemiya, T. Fuda, T. Tamura, T. Kuriiwa, A. Kamegawa, M. Okada, Mater. Trans. JIM 40 (1999) 871–874.
[8] T. Fuda, K. Matsumoto, Y. Tominaga, T. Tamura, T. Kuriiwa, A. Kamegawa, M. Okada, Mater. Trans. JIM 41 (2000) 577–580.
[9] Y. Tominaga, K. Matsumoto, T. Fuda, T. Tamura, T. Kuriiwa, A. Kamegawa, H. Takamura, M. Okada, Mater. Trans. JIM 41 (2000) 617–620.
[10] M. Okada, T. Kuriiwa, T. Tamura, H. Takamura, A. Kamegawa, J. Alloys Comp. 330–332 (2002) 511–516.
[11] T. Tamura, A. Kamegawa, H. Takamura, M. Okada, Mater. Trans. 42 (2001) 1862–1865.
[12] T. Tamura, Y. Tominaga, K. Matsumoto, T. Fuda, T. Kuriiwa, A. Kamegawa, H. Takamura, M. Okada, J. Alloys Comp. 330–332 (2002) 522–525.
[13] T. Tamura, A. Kamegawa, H. Takamura, M. Okada, Mater. Trans. 43 (2002) 410–413.
[14] A. Kamegawa, K. Shirasaki, T. Tamura, T. Kuriiwa, H. Takamura, M. Okada, Mater. Trans. 43 (2002) 470–473.
[15] K. Shirasaki, T. Tamura, T. Kuriiwa, T. Goto, A. Kamegawa, H. Takamura, M. Okada, Mater. Trans. 43 (2002) 1115–1119.
[16] K. Shirasaki, T. Kuriiwa, T. Tamura, A. Kamegawa, H. Takamura, M. Okada, Mater. Trans. 43 (2002) 1173–1177.
[17] T. Tamura, M. Hatakeyama, T. Ebinuma, A. Kamegawa, H. Takamura, M. Okada, Mater. Trans. 43 (2002) 1120–1123.
[18] T. Tamura, T. Kazumi, A. Kamegawa, H. Takamura, M. Okada, Mater. Trans. 43 (2002) 2753–2756.
[19] T. Kazumi, T. Tamura, A. Kamegawa, H. Takamura, M. Okada, Mater. Trans. 43 (2002) 2748–2752.